SELF-HEALING OF GALVANIC ZINC COATINGS IN THE PRESENCE OF NANO-AGGREGATES

D.A. Koleva[1], P. Taheri[2], N. Boshkov[3], P. Petrov[4],
K.van Breugel[1], J.H.W. de Wit[2] and J.M.C.Mol[2]
[1,2]Delft University of Technology, The Netherlands
[1]Faculty of CiTG, Department Materials & Environment; Stevinweg 1, 2628 CN, Delft;
[2]Faculty 3mE, Department Surfaces & Interfaces, Mekelweg 2, 2628 CD Delft.
[3]Institute of Physical Chemistry, [4]Institute of Polymers
[3,4]Bulgarian Academy of Sciences, Acad. G. Bonchev, bl.11, Sofia 1113, Bulgaria

Abstract

The corrosion behavior of galvanic Zn and nano-composite Zn in the corrosion medium of 5% NaCl solution was investigated. The main points of discussion are the superior performance of the Zn-composite coating and the "self-healing" effects in the presence of nano-aggregates (0.5 g/l stabilized core-shell micelles). The increased corrosion resistance of the composite Zn coating was evaluated by electrochemical techniques (PDP, SVET) and surface analysis (XPS, SEM) of the coatings after treatment.

Key words: *galvanic zinc; nano-aggregates; SVET; SEM; XPS*

1. INTRODUCTION

Protective coatings have traditionally been developed possessing one or more functionalities: impermeable physical barrier; passivation (conversion); cathodic protection; galvanic action of the coating as a sacrificial material etc. Whereas these strategies perform well to prevent corrosion damage, none of these work particularly well when the coating has been physically breached or when the sacrificial metal has been exhausted. Novel materials (as the hereby proposed coatings) need to possess all the characteristics of the current state of the art protective coatings, with the additional function of self-healing upon damage.

Electrodeposited zinc coatings are widely used in practice for preventing the corrosion of steel or improving corrosion resistance. Various methods and techniques are available for improving the zinc coatings performance e.g. alloying with other metals [1-10], conversion coatings, based mainly on environmentally friendly compounds [11-13] and more recently, composite coatings, incorporating micro- or nano-sized polymeric aggregates [14-16]. Another approach is the electrodeposition of nanocrystalline coatings by using selected organic additives or pulse deposition techniques [17]. The corrosion resistance of the zinc layer is in correlation with and depending on the morphology and crystallographic orientation in the deposit [18-20]. These conditions and in particular grain refinement of the zinc layer, may be achieved by means of incorporating polymeric nano-sized aggregates (core-shell architectures), which on one hand act as new nucleation sites and on the other hand, increase the corrosion resistance of the zinc layers in aggressive environment, due to the amphiphilic nature of the used polymer.

An improvement of the corrosion resistance of a zinc coating, with incorporated within the electro-deposition process polymeric nano-aggregates (concentration of only 1 g/l in the starting electrolytes) was previously achieved: the investigated coatings contained poly (ethylene oxide) – b – poly (propylene oxide) – b poly (ethylene oxide) micelles (PEO-PPO-PEO) [21] or polymer nano-aggregates from the amphiphilic tri-block copolymer poly (2 - hydroxyethyl methacrylate) – b – poly (propylene oxide) – b – poly (2 - hydroxyethyl methacrylate) ($PHEMA_{15}PPO_{34}$ $PHEMA_{15}$) [22]. This paper reports on the corrosion behavior and surface properties of galvanic and nano-composite Zn coatings, the latter containing twice lower (compared to previous research) concentration of nano-aggregates - Poly (ethylene oxide)-block-polystyrene (PEO_{113}-b-PS_{218}) micelles in concentration of 0.5 g/l to the starting electrolyte. A more detailed electrochemical behavior of these coatings, compared to galvanic Zn, as well microscopical, and XRD analysis are reported in [22,23]. This paper reports on electrochemical response in correlation with XPS analysis and can be considered as a first step for on-going research on self-healing galvanic coatings in the presence of nano-aggregates.

2. EXPERIMENTAL

2.1 Materials

Galvanic coatings: Both zinc (Zn) and composite zinc (ZnP) coatings were electrodeposited on a steel substrate (low carbon steel, surface area of $1cm^2$) from slightly acidic sulfate-chloride electrolyte with the following composition: 150 g/l $ZnSO_4.7H_2O$, 30 g/l NH_4Cl, 30 g/l H_3BO_3, additives AZ-1 (wetting agent) 50 ml/l and AZ-2 (brightener) 10 ml/l. For the ZnP coating, the electrolyte also contains the previously stabilized in demi-water PEO_{113}-b-PS_{218} micelles (concentration of the micelles in the electrolyte is 0.5 g/l). The electrodeposition conditions were realized at current density of 2 A/dm^2, pH 4.5-5.0, t^o – 22°C, no stirring or agitation. The coating thickness for both Zn and ZnP layers was approximately 8 μm. The results from the electrochemical tests are an average of 3 replicates per type and per stage. Corrosion medium was 5% NaCl solution.

Polymeric micelles: Poly (ethylene oxide) – block - polystyrene (PEO_{113}-b-PS_{218}) diblock copolymer was synthesized by atom transfer radical polymerization (ATRP) employing the macro-initiator technique. The polymeric core-shell micelles were

further formed by dissolving PEO_{113}-b-PS_{218} diblock copolymer in dioxane and subsequent dialysis against demi water. Uniform micelles with spherical morphology were observed by transmission electron microscopy (TEM) and atomic force microscopy (AFM), Fig.1a)c). Dynamic light scattering measurements (DLS, Fig.1b) showed an apparent hydrodynamic radius Rh = 60 nm.

2.2. Methods

Potentio-dynamic polarization (PDP) was performed in the range of -0.15 V to +1.2 V vs OCP at scan rate of 1mV/s (in a common three-electrode electrochemical cell, all readings are versus SCE reference electrode, using EcoChemie Autolab).

Scanning vibrating electrode technique (SVET) measurement: the instrument used was from Applicable Electronics (Forestdale, MA); the scanned area was 3.4 × 2.6 mm at a distance of 100 μm between the samples surface and the microelectrode.

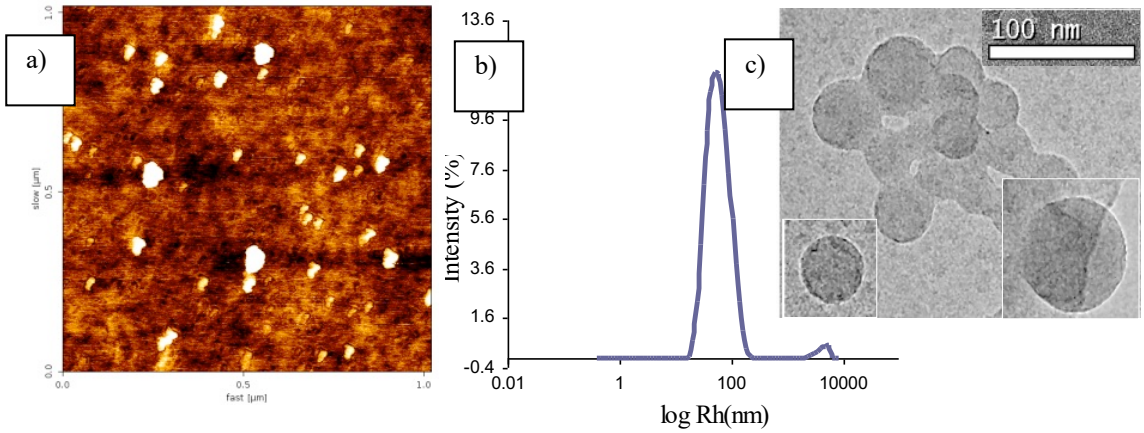

Fig.1. PEO_{113}-b-PS_{218} micelles, defined in demi water (before coatings' electrodepo-sition), using: a) AFM (liquid sample); b) DLS and c) TEM

Microscopic investigation (SEM), using ESEM Philips XL30.

XPS measurements were carried out in the UHV chamber of the electron spectrometer ESCALAB-MkII (VG Scientific) with a base pressure of about 1.10-10 mbar (during the measurement 1x10-9 mbar). The photoelectron spectra are obtained using un-monochromatized AlKα (hν=1486.6 eV) radiation. The instrumental resolution measured as the full width at a half maximum (FWHM) of the Ag3d5/2, photoelectron peak is about 1 eV. The energy scale is corrected to the C1s - peak maximum at 285 eV for electrostatic sample charging.

3. RESULTS AND DISCUSSION

3.1. Corrosion behavior of Zn and nano-composite ZnP

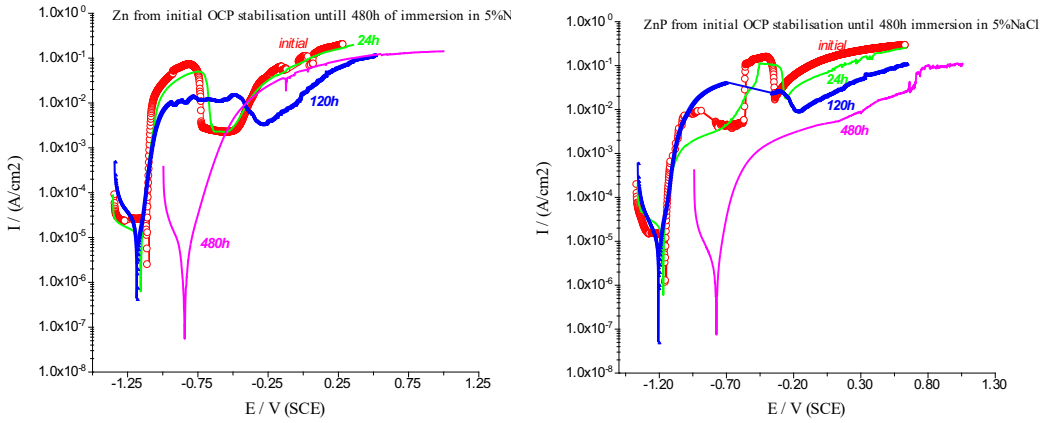

Fig. 2 Overlay of potentio-dynamic scans for Zn (left) and ZnP (right) for the different intervals from initial until 480h treatment in 5%NaCl.

Figures 2 presents the potentio-dynamic polarization curves for Zn (left) and composite ZnP (right) coatings (as an overlay of scans for different immersion times), starting with scans after initial immersion and OCP stabilization, (initial); 24h, 120h and 480h. Initially the ZnP coating exhibits lower corrosion current density and prolonged anodic region after corrosion potential, accounting for impeded anodic process i.e. higher corrosion resistance. After 24h, corrosion current density for both coatings is similar, the ZnP coating however, exhibiting significantly lower anodic currents immediately after corrosion potential and fluctuations thereafter. Further, after prolonged immersion times, although corrosion potential of Zn and ZnP is similar, the corrosion resistance for the ZnP coating is higher, compared to the Zn coating. Fig.3 depicts the calculated polarization resistance values (Rp in kOhm.cm2) over the investigated period and the recorded open circuit potentials, showing a more distinguished ennoblement for the ZnP coating. Figures 2 and 3 clearly show the superior performance of the composite coating, especially with prolonged treatment, in the highly aggressive environment of 5% NaCl.

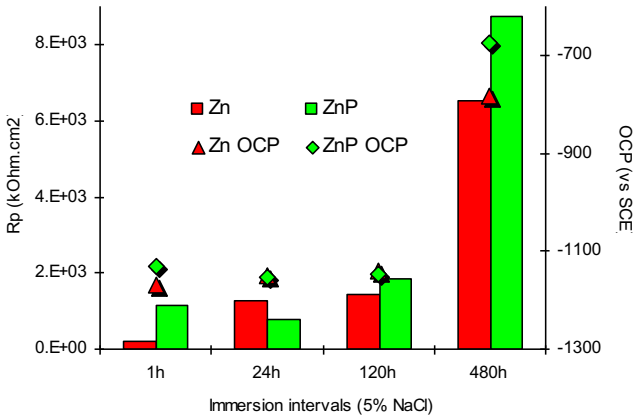

Fig.3 Polarization resistance values and OCP from 1h to 480h immersion in 5%NaCl

The corrosion behavior, recorded with PDP tests is supported by SVET measurements (Fig.4), (the current density maps present the local current evolution over the couple ZnP|Zn as schematically shown in Fig.4a). The initially more active anodic behavior for the ZnP coating (Fig.4a)b) gradually changes to cathodic (Fig.4c) and reverse of cathodic/anodic activity (Fig.4d)-f)), whereas the Zn coating generally exhibits anodic activity, starting after 4h of treatment. After 24h, both Zn and ZnP exhibit significantly reduced anodic currents (Fig.4f); further on (32h and 48h) anodic dissolution again increases for both coatings, however with lower currents and a more uniform local current distribution for the ZnP coating. The mechanisms are denoted to formation of corrosion products with low solubility (zinc oxides, hydroxides and oxy-hydroxy chlorides) and barrier effects (blocking the surface), the latter being with a reversible mechanism for this type of coatings and the investigated corrosion medium.

When the composite coating is exposed to NaCl solution, there is an accelerated corrosion rate at earlier stages of immersion (compared to the pure galvanic zinc), denoted to opening gaps between the particle and the zinc matrix (in addition to the underneath voids, formed in the process of deposition, as previously discussed). Consequently, earlier stages corrosion rate of the composite coating ends up higher, compared to galvanic zinc (Fig. 3, Fig.4a)b)d). With time of treatment, the corrosion process slows down significantly and further the composite coating exhibits much higher corrosion resistance. This will be the case, since the preferential corrosion around the polymer particles takes place intensively (fresh surface) but on a very small area, compared to the total surface. This makes a large

ratio of anodic/cathodic areas and once the fresh anodic areas (comparatively too small) are covered with products, the corrosion rate will decrease significantly. The process is of course supported by the hydrophobic parts of the particles in the film, which additionally enhances the barrier properties of the coating. The latter mechanisms can be considered as a kind of "self-healing" of the composite ZnP coating.

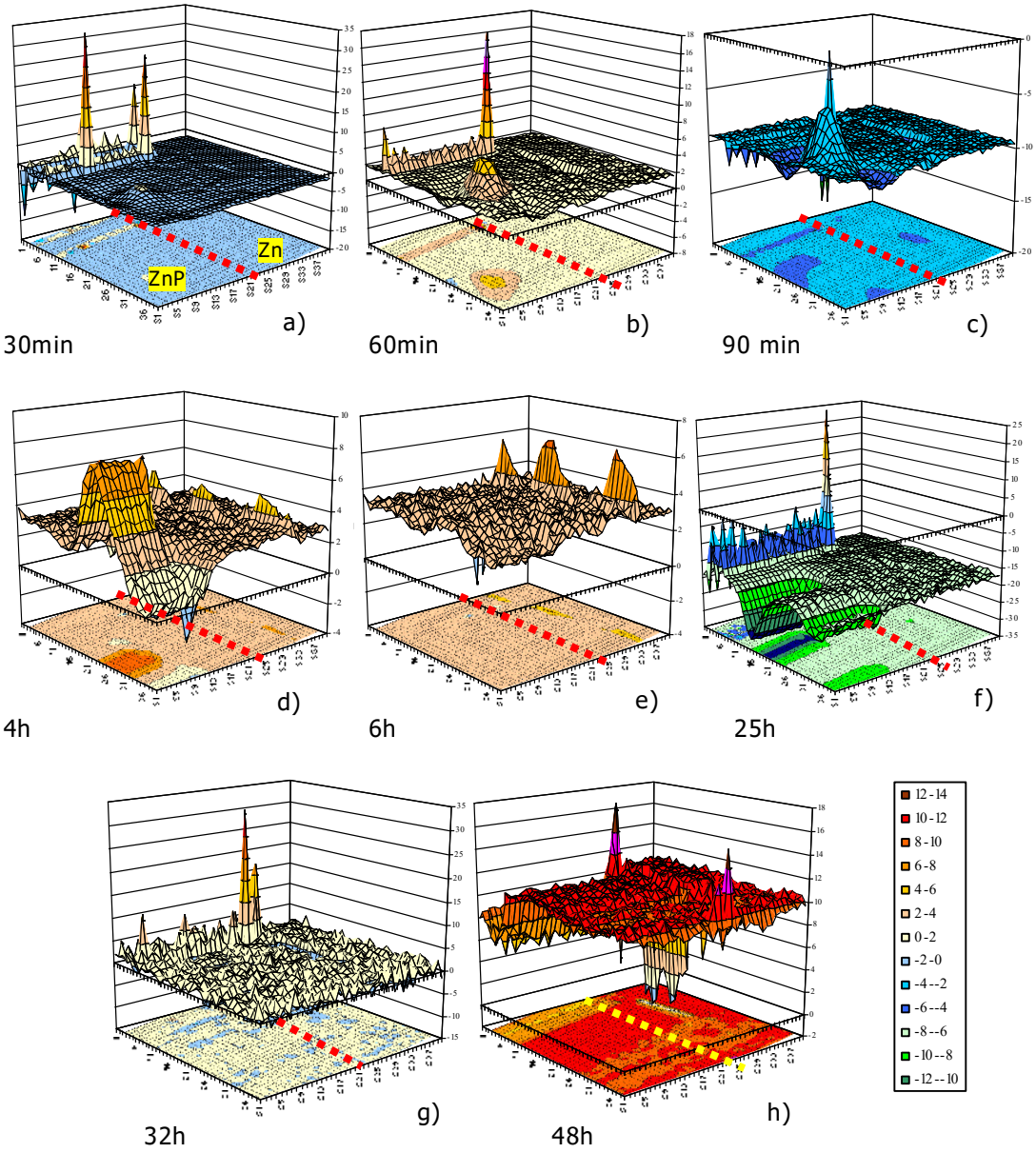

Fig.4. Current density maps (SVET measurements) for Zn and ZnP at different time intervals (measurement in 0.001M NaCl)

3.2. Surface analysis

The above discussed mechanisms for the state, composition and reversible mechanisms, especially for the ZnP coating are clarified by XRD, XRF, EDX measurements (not hereby presented, reported in [22,23]. In what follows, XPS and SEM investigation support the hereby discussed electrochemical behavior.

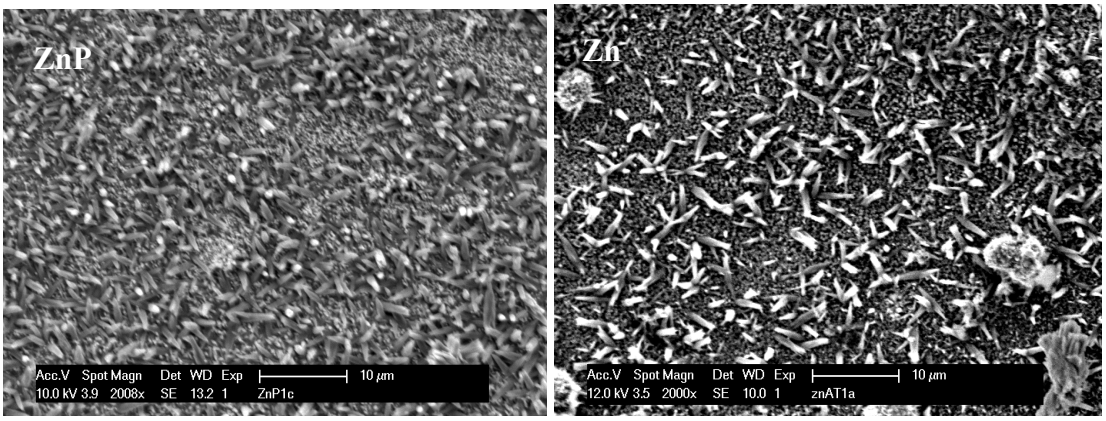

Fig.5. SEM micrographs of the product layers, formed after 48h immersion in 5% NaCl for ZnP (left) and Zn (right).

Figure 5 presents the morphological observation of both coatings after 48h treatment in 5% NaCl. As seen from the micrographs, although similar formations are present in both coatings, the surface of the ZnP sample is more uniform and compact (Fig.5 left), whereas the Zn coating presents a non-compact layer and non-uniformly distributed larger formations (ZnO and $Zn_5(OH)_8Cl_2.H_2O$). Further XPS analysis supports the observed electrochemical behavior and morphological observations (on these latter more details can be referred to [22,23]).

XPS Zn patterns: As seen from Table 1, similar amounts of zinc for both specimens were derived. In such a case the newly appeared corrosion products together with the retained (non-corroded) part of the coating play an important role for the protective properties of the layer. The zinc peak of the composite is of higher intensity and is shifted to greater binding energy values (E_{bind} 1022,1 eV) compared to the peak of the pure zinc deposit (E_{bind} 1021,7). This is denoted to the presence of Zn^{2+}-ions coordinated by OH^- groups and Cl^- anions so the main compounds in the composite seem to be $Zn(OH)_2$ and $ZnCl_2$. Considering the corrosion medium of NaCl, and the higher binding energy (E_{bind}) the appearance of $Zn_5(OH)_8Cl_2.H_2O$ – zinc hydroxide chloride (ZHC), containing both $Zn(OH)_2$ and $ZnCl_2$ is expected. The presence of ZHC generally increases the protective ability of the coating (higher diffusion limitations and barrier effects). In contrast, the pure Zn coating contains more ZnO (the peak shoulder is shifted to lower E_{bind} values, Fig. 4 (left), leading to lower $Zn(OH)_2$ and $ZnCl_2$ content (and ZHC respectively). The observation denotes for greater surface heterogeneity on the zinc sample that is unfavourable from a corrosion view point i.e. zinc oxides have protective properties if uniformly distributed. If this is not the case, additional microstructural interactions appear and the protective properties are reduced.

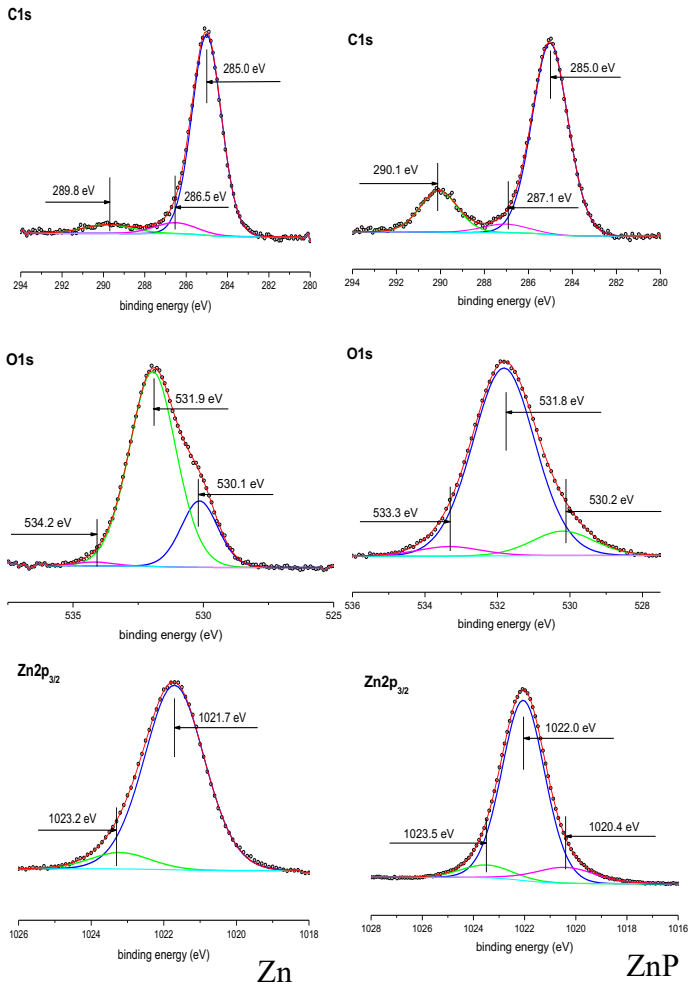

Table 1 – Summary XPS results

	at. %	Binding Energy, eV	Relevant compounds
Zn specimen			
Zn	21	1021,7	ZnO, $Zn(OH)_2$, $ZnCl_2$ $Zn_5(OH)_8Cl_2.H_2O$
O	36	531,9	$Zn(OH)_2$
		530,1	ZnO
Cl	2	199,2	$ZnCl_2$
		200,3	$ZnCl_2$, $Zn_5(OH)_8Cl_2.H_2O$
C	41	286,5	$ZnCO_3$
		290,0	
ZnP specimen			
Zn	23	1022,1	$Zn(OH)_2$, $ZnCl_2$ $Zn_5(OH)_8Cl_2.H_2O$
O	39	531,8	$Zn(OH)_2$
Cl	4	199,2	$ZnCl_2$
		200,3	$ZnCl_2$, $Zn_5(OH)_8Cl_2.H_2O$
C	35	287,3	$ZnCO_3$
		290,1	

Fig.6 XPS analysis: (left) experimental results (C1s, O1s and Zn2p3/2); Table 1: XPS results summary and quantification of main compounds (right).

XPS Oxygen patterns: As given in Table 1, the oxygen content for the composite ZnP is higher i.e. this sample is more oxidized. The main oxygen peaks for both Zn and ZnP appear at almost one and the same E_{bind} values (531,9 and 531,8 eV) the peak for ZnP being with greater intensity, corresponding to the values in Table 1. The Zn sample shows an oxygen peak (and shoulder) with lower intensity at E_{bind} value of 530, 1 eV that is characteristic for ZnO (most likely both samples contain H_2O as well, since their patterns cover the relevant binding energy). These observations confirm that the protective film on the composite ZnP specimen is more homogeneous, practically containing mainly ZHC while in the case of the pure zinc specimens, ZnO is non-uniformly distributed among the layer of newly formed corrosion products. This will lead to relatively higher activity on the surface as well as to lower protective ability of the Zn coating, compared to composite ZnP coating.

XPS Chloride patterns: As seen from Table 1 the Cl amount (not presented in the form of XPS pattern) is higher in the case of the composite zinc (ZnP). On one hand this fact is unfavorable for the protective properties of the coating (possible activity of the chloride ions); on the other hand, this result denotes for higher ZHC amounts present on the surface, meaning greater barrier effects.

XPS Carbon patterns: Higher amount of carbon appears on the pure zinc sample. The peaks are characteristic for C-O bond and CO_3^{2-}containing compounds (most probably $ZnCO_3$ and/or $ZnHCO_3$). For comparison, the products of solubility value of $ZnCO_3$ is about 10^{-10} or 10^{-11} that is much lower compared to $Zn(OH)_2$ – 10^{-17} - or ZHC – 10^{-14} i.e. higher carbonates content (as in Zn specimens) will not protect the substrate, as would be in the case of accumulated $Zn(OH)_2$ and ZHC (as in the ZnP specimens).

4. CONCLUSIONS

In conclusion, the electrochemical measurements and surface analysis reveal the superior performance of the composite ZnP coating in the highly aggressive medium of 5% NaCl, especially with prolonged immersion time. The higher corrosion resistance of the ZnP coating is denoted to an enhanced barrier effect of the coating, which is due to the presence of the polymer nano-aggregates themselves, but is also denoted to a kind of "self-repairing" mechanism, resulting from the specific properties of the aggregates' core and shell in chloride containing environment. Consequently, a more uniform layer of well compact and stable products is formed (mainly ZnO) in the ZnP coating, and therefore a higher corrosion resistance, compared to the Zn coating is observed.

REFERENCES

1. Lodhi Z.F., Mol J.M.C., Hovestad A., Terryn H., de Wit J.H.W., *Surface and Coatings Technology,* 2007; 202, 84.

2. Boshkov N., Petrov K., Vitkova S., Nemska S., Raichevski G., *Surface and Coatings Technology*, 2002; 157, 171.

3. Boshkov N., Petrov K., Kovacheva D., Vitkova S., Nemska S., *Electrochim. Acta* 2005; 51, 77.

4. Mangolini F., Magagnin L., Cavallotti P.L., *J. Electrochem. Soc*. 2006; 153, C623.

5. Ganesan P., Kumaraguru S.P., Popov B.N., *Surf.&Coat.Technol*. 2006; 201, 3658.

6. Mouanga M., Ricq L., Douglade J., Berçot P., *J.Appl.Electrochem*. 2007; 37, 283.

7. Rosalbino F., Angelini E., Maccio D., Saccone A., Delfino S., *Electrochim. Acta* 2007; 52, 7107.

8. Neto P.D.L., Correia A.N., Colares R.P., Araujo W.S., *J. Brazilian Chem Soc*. 2007; 18, 1164.

9. Carpenter D.E.O.S., Farr J.P.G., *Trans.Inst.Metal Finish*. 2007; 85, 298.

10. Shivakumara S., Arthoba Naik Y., Achary G., et al., Ind. *J.Chem.Technol*. 2008; 15, 29.

11. Biestek T., Weber J., Conversion Coatings, Portcullis Press Ltd., Redhill, 1976.

12. Twite R. L., Bierwagen G. P., *Prog.Org.Coat*. 1998; 33, 91.

13. Rafaey S. A. M., Abd El-Rehim S. S., Taha F., et al. *Appl. Surf. Sci*. 2000; 158, 190.

14. Hovestad A.,.Heesen R.J.C.H.L, Janssen L.J.J., *J.Appl. Electrochem*. 1999; 29, 331.

15. Koleva D. A., Boshkov N., Raichevski G., Veleva L., *Trans. Instit. Metal Finish*. 2005; 83, 188.

16. Boshkov N., Tsvetkova N., Petrov P., Koleva D., Petrov K., et al. *Appl.Surf. Sci*. 2008; 254, 5618.

17. Li M., Luo S., Qian Y., Zhang W., Jiang L., Shen J., *J. Electrochem.Soc*. 2007; 154, D567.

18. Seré P. R., Culcasi J. D., Elsner C. I., Di Sarli A. R., *Surf.& Coat. Technol*. 1999; 122, 143.

19. Park H., Szpunar J.A., *Corros. Sci*. 1998; 40, 525.

20. Budevski E., Staokov G., Lorenz W. J., *Electrochim.Acta*. 2000; 45, 2559.

21. Koleva D.A., Zhang X., Petrov P., Boshkov N., et al. *ECS Trans*. 2008; 11, 27.

22. Koleva D.A., van Breugel K., Petrov P., et al. in:EUROCORR'08, Edinburgh UK, 7-11 Sept 2008.

23. Koleva D.A., Boshkov N., Bachvarov V., Zhan H., de Wit J.H.W., van Breugel K., Mol J.M.C., Application of PEO113-b-PS218 nano-aggregates for improved protective characteristics of composite zinc coatings in chloride containing environment, submitted to *Surf.Coat.Technol*., 2009